Hindawi Publishing Corporation
The Scientific World Journal
Volume 2014, Article ID 136340, 6 pages
http://dx.doi.org/10.1155/2014/136340

Research Article

100 nm AlSb/InAs HEMT for Ultra-Low-Power Consumption, Low-Noise Applications

Cyrille Gardès, Sonia Bagumako, Ludovic Desplanque, Nicolas Wichmann, Sylvain Bollaert, François Danneville, Xavier Wallart, and Yannick Roelens

Institut d'Électronique de Microélectronique et de Nanotechnologie (IEMN), UMR CNRS 8520, Université Lille I, BP 60069, 59652 Villeneuve d'Ascq Cedex, France

Correspondence should be addressed to Cyrille Gardès; cyrille.gardes@iemn.univ-lille1.fr

Received 30 August 2013; Accepted 5 January 2014; Published 23 February 2014

Academic Editors: Y.-S. Lin, J. F. Paris, and J.-H. Park

Copyright © 2014 Cyrille Gardès et al. This is an open access article distributed under the Creative Commons Attribution License, which permits unrestricted use, distribution, and reproduction in any medium, provided the original work is properly cited.

We report on high frequency (HF) and noise performances of AlSb/InAs high electron mobility transistor (HEMT) with 100 nm gate length at room temperature in low-power regime. Extrinsic cut-off frequencies f_T/f_{max} of 100/125 GHz together with minimum noise figure NF_{min} = 0.5 dB and associated gain G_{ass} = 12 dB at 12 GHz have been obtained at drain bias of only 80 mV, corresponding to 4 mW/mm DC power dissipation. This demonstrates the great ability of AlSb/InAs HEMT for high-frequency operation combined with low-noise performances in ultra-low-power regime.

1. Introduction

Though the best high frequency performances are obtained for InAlAs/InGaAs HEMT technology which is more mature [1], AlSb/InAs HEMTs are potentially excellent candidates for low-voltage, low-power consumption operation in the case of high-speed analog and digital applications [2]. AlSb/InAs heterostructures are grown since the 1980s [3, 4], but AlSb/InAs HEMT with noticeable RF figures-of-merit and amplifiers with interesting low-noise performances have only been obtained since the last ten years [5, 6].

The best extrinsic f_T of 303 GHz has been reached for a transistor with 120 nm gate length at drain bias of 0.44 V [7]. The main modifications regarding our previous work [7, 8] lie in an optimization of heterostructure growth conditions [9], no ohmic cap layer [10], and the use of alternative metallic gate stack [11]. With this technology, the highest combination of cut-off frequencies obtained simultaneously for AlSb/InAs HEMTs has recently been shown at V_{ds} = 360 mV [10], beyond previous f_T/f_{max} record of 260/280 GHz reported for 100 nm HEMT at V_{ds} = 400 mV [12]. Cut-off frequencies f_T/f_{max} of 290/335 GHz were obtained for a 120 nm HEMT. We presently focus on HEMT operation in mobility regime (V_{ds} = 80 mV) in which we will demonstrate that no impact ionization occurs. In these low drain bias conditions, corresponding to ultra-low-power dissipation, previous works report f_T/f_{max} of 112/107 GHz for (V_{ds} = 0.1 V; P_{DC} = 4.3 mW/mm) [5] and f_T/f_{max} of 143/115 GHz at (V_{ds} = 0.1 V; P_{DC} = 9.9 mW/mm) [7]. In this study, we present a full set of characteristics at V_{ds} = 80 mV regarding DC, HF, and noise performances, extracting RF figures-of-merit, extrinsic and intrinsic parameters, and noise parameters obtained from small-signal equivalent circuit with noise sources.

2. Heterostructure and Device Fabrication

2.1. Heterostructure. The AlSb/InAs heterostructure was grown by molecular beam epitaxy on 3-inche semi-insulating GaAs substrate. A thick AlSb buffer is used to accommodate the large lattice mismatched between 6.1 Å materials and GaAs substrate. Then, the structure consists of a 120 Å InAs channel, a 65 Å AlSb spacer, a Te δ-doping plane, and a composite Schottky barrier with a 25 Å $Al_{0.8}Ga_{0.2}Sb$ layer and a 50 Å $Al_{0.5}In_{0.5}As$ layer (Figure 1). The $Al_{0.5}In_{0.5}As$ layer in the composite Schottky barrier avoids oxidation of $Al_{0.8}Ga_{0.2}Sb$ with air exposure and acts as a hole barrier [13]. Hall measurements at room temperature exhibit a sheet

Protection layer	$Al_{0.5}In_{0.5}As$	50 Å
Barrier layer	$Al_{0.8}Ga_{0.2}Sb$	25 Å
δ-doping plane	Te 4.5×10^{12} cm^{-2}	
Spacer layer	AlSb	65 Å
Channel layer	InAs	120 Å
Buffer layer	AlSb	500 Å
Buffer layer	$Al_{0.8}Ga_{0.2}Sb$	2500 Å
Buffer	AlSb	15000 Å
S.I. substrate	GaAs	

Figure 1: AlSb/InAs heterostructure.

carrier density of 1.5×10^{12} cm^{-2} and electron mobility of 26000 cm^2/(Vs), giving sheet resistance of 160 Ω/□.

2.2. Device Fabrication. HEMTs fabrication starts with ohmic contact evaporation of Pd/Pt/Au after e-beam lithography, followed by rapid thermal annealing at 275°C. Despite the absence of highly doped cap layer in the heterostructure, contact resistance, obtained by transmission-line model measurements, is still below 0.05 Ω·mm. Schottky T-gate is realized using bilayer resist e-beam lithography process and Mo/Pt/Au metallization. Then, Ti/Au bonding pads are evaporated. Finally, the active area is defined by chemical deep mesa isolation using HF/H_2O_2 solution to completely remove the AlSb buffer, leading to air-bridge gate. Device features are a two-finger 100 nm long gate with 2×25 μm transistor width (Figure 2). Source-drain spacing is 1.2 μm.

3. Static and Dynamic Measurements

Drain current-voltage characteristics are plotted in Figure 3. Pinch-off voltage is −1.0 V. Maximum drain currents are 220 mA/mm and 620 mA/mm for drain bias of 80 mV and 240 mV, respectively. These are similar to our previous results [7, 8] despite the higher sheet resistance of the heterostructure and the higher source-drain spacing in the present device.

HF measurement setup consists in a 67 GHz Agilent PNA for S-parameters on-wafer measurements and an Agilent HP4142 generator for DC biasing. Extrinsic current gain $|H_{21}|^2$ and unilateral power gain U for V_{ds} = 80 mV and V_{ds} = 240 mV at peak f_T are presented in Figure 4. Cut-off frequencies (f_T, f_{max}) obtained simultaneously at V_{ds} = 80 mV are (108 GHz, 129 GHz) for power dissipation P_{DC} = 5 mW/mm and (232 GHz, 250 GHz) at V_{ds} = 240 mV for P_{DC} = 60 mW/mm. P_{DC} is calculated as $V_{ds} \times I_{ds}$, with power consumption in the gate being negligible.

In Figure 5, the evolution of extrinsic cut-off frequencies is plotted as a function of P_{DC} for V_{ds} = 80 mV and V_{ds} = 240 mV. This evidences the ability of AlSb/InAs HEMT for RF performances in low drain bias regime. In fact, (f_T, f_{max}) are (100 GHz, 125 GHz) for P_{DC} = 4 mW/mm at V_{ds} = 80 mV. The DC power consumption at V_{ds} = 240 mV for reaching the same cut-off frequencies is, respectively, 30 mW/mm and 22 mW/mm. Consequently, to get the same RF performances in more standard drain bias conditions, power consumption must be at least 5 times higher.

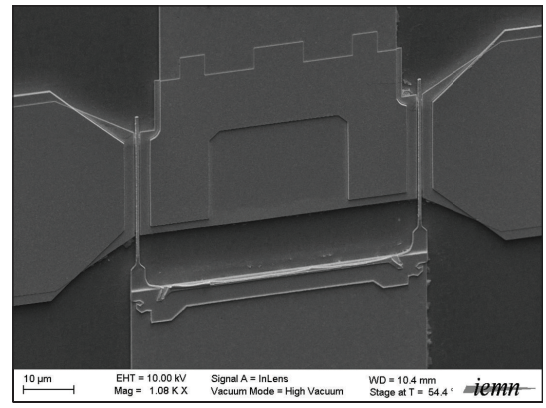

Figure 2: 100 nm AlSb/InAs HEMT.

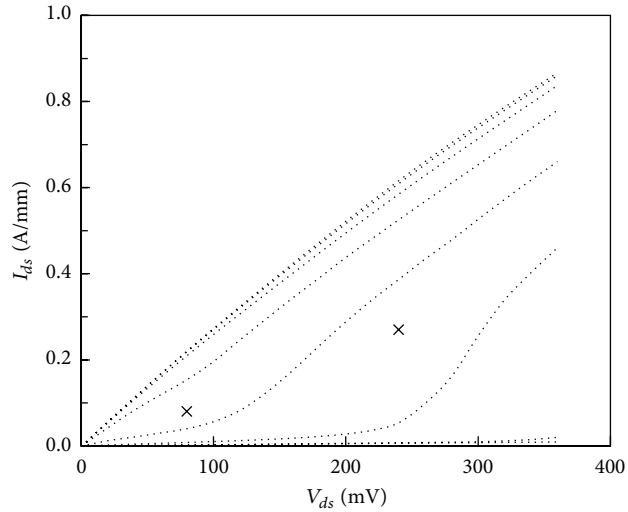

Figure 3: Drain current-voltage characteristic of 100 nm AlSb/InAs HEMT. V_{gs} is varying from 0 V to −1.4 V with −0.2 V step. (Crosses are polarisation conditions for measurements at peak f_T).

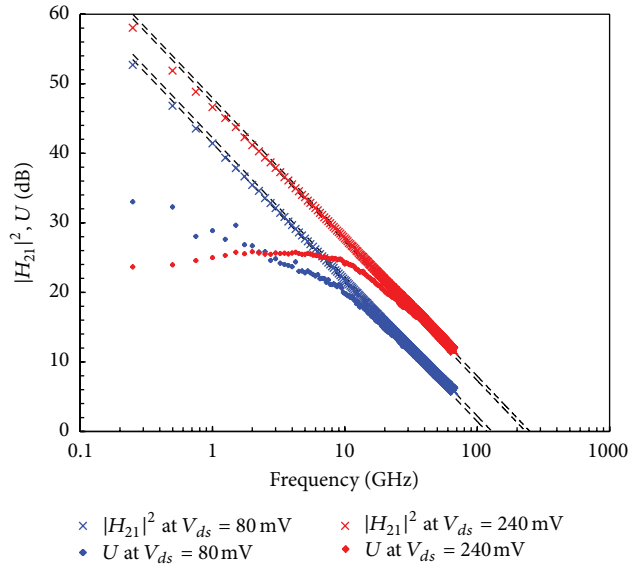

Figure 4: f_{max} and f_T extrapolated from Mason's unilateral gain U and current gain $|H_{21}|^2$ for V_{ds} = 80 mV and V_{ds} = 240 mV.

Table 1: Small-signal equivalent circuit parameters for V_{ds} = 80 mV and V_{ds} = 240 mv at peak f_T.

V_{ds} (mV)	R_G (Ω/mm)	R_D (Ω·mm)	R_S (Ω·mm)	g_m (S/mm)	g_d (S/mm)	C_{gs} (fF/mm)	C_{gd} (fF/mm)	g_{m2} (S/mm)	R_{gg} (k Ω)
80	74	0.11	0.11	0.75	0.73	468	327	0.007	80
240	74	0.11	0.11	1.36	0.72	584	259	1.47	12

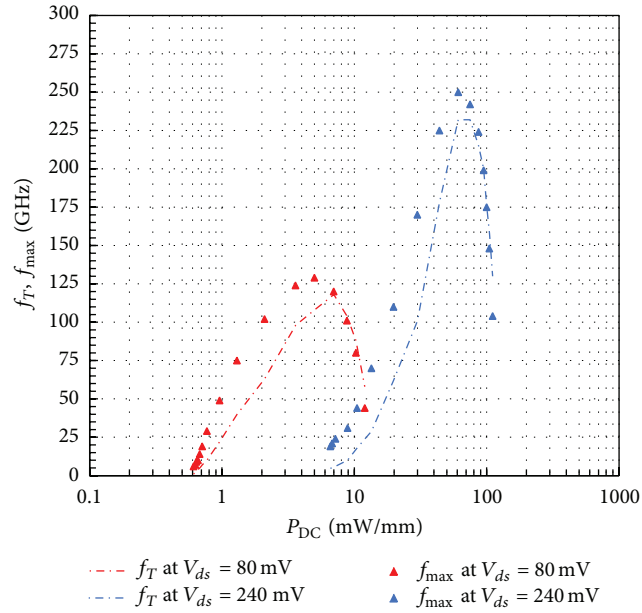

Figure 5: Extrapolated (f_T, f_{max}) plotted as a function of DC power consumption calculated as $V_{ds} \times I_{ds}$.

Finally, intrinsic and extrinsic parameters have been extracted from the small-signal equivalent circuit (SSEC) presented in Figure 6.

Resistance R_{gg} parallel to C_{gs} and current source g_{m2} parallel to output conductance g_d to account, respectively, for gate leakage current and impact ionization have been added to the classical model. Indeed, there is impact ionization in AlSb/InAs HEMT at high drain bias with an increase of gate current and a typical bell-shape of the I_{gs}-V_{gs} characteristic [14], which is a signature of impact ionization in DC measurements. With RF characterization, impact ionization results in S_{22} parameter evolving from inductive to capacitive behaviour with increasing frequency as can be seen for V_{ds} = 240 mV in Figure 7. In the literature, this phenomenon in HEMTs has been modelised with a low-pass filter [15]. We prefer to introduce an additional current source g_{m2} controlled by gate-drain voltage as realized by Isler [16] to account for impact ionization effects. This model allows to perfectly fit scattering parameters at V_{ds} = 80 mV and V_{ds} = 240 mV as shown in Figure 7.

Parameters extracted from the SSEC at peak f_T are presented in Table 1. R_{gg} is much higher at V_{ds} = 80 mV compared to V_{ds} = 240 mV, which is relevant of much lower gate leakage current, and g_{m2} is negligible at V_{ds} = 80 mV, which stresses that there is no impact ionization at this drain voltage.

4. Noise Measurements

Regarding low impact ionization occurring at V_{ds} = 80 mV as shown above with RF wideband measurements, SSEC with noise sources as presented in Figure 8 is used. For the sake of simplicity, there is no current source accounting for impact ionization since extracted value of g_{m2} at V_{ds} = 80 mV is negligible. As a consequence, no additional noise source, which should probably be correlated with output noise current or even input noise voltage, is required for extraction of accurate parameters values. We extracted the following noise parameters using F_{50} method [17]: minimum noise figure NF_{min}, associated gain G_{ass}, noise equivalent resistance R_n, and output noise temperature T_{out} at 12 GHz (Figures 9 and 10). NF_{min} is 0.5 dB and G_{ass} is 12 dB for 4 mW/mm power dissipation. As a comparison, we should quote results obtained by Ma et al. [5] for 2 × 20 μm HEMT with NF_{min} above 0.5 dB at 12 GHz in the "best bias conditions for minimum noise figure." The present results should also be compared with similar NF_{min} and G_{ass} reported in literature for AlSb/InAs HEMTs but with 50% higher DC power consumption of 6 mW/mm at V_{ds} = 200 mV [6, 18]. In the present case, at V_{ds} = 80 mV, NF_{min}, and G_{ass} are optima for P_{DC} = 4 mW/mm and it is important to underline that it would be impossible to reach these noise performances at

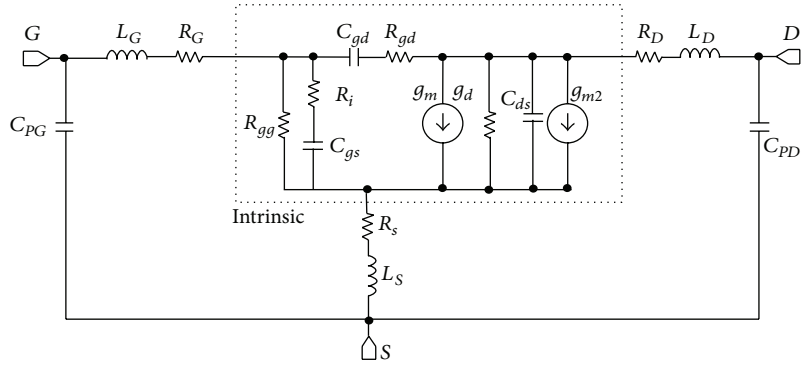

Figure 6: Small-signal equivalent circuit tacking into account gate leakage current (R_{gg}) and impact ionisation (g_{m2}).

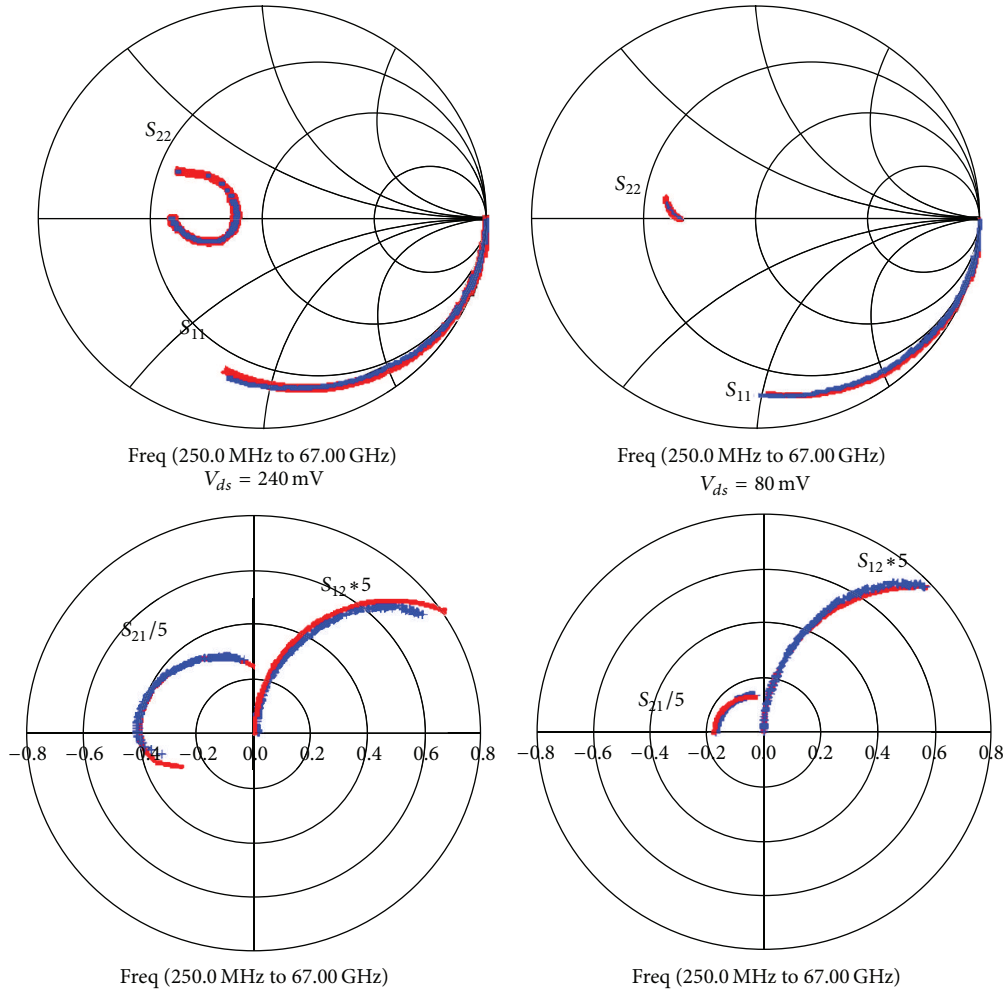

Figure 7: S-parameters measured (blue dots) and simulated (red curves) at V_{ds} = 80 mV and V_{ds} = 240 mV.

V_{ds} = 240 mV with such low-power consumption. Despite an accurate extraction of noise parameters under high drain bias is not done here, the element values would obviously be degraded due to the higher gate voltage required to operate in low-power regime, which would increase shot noise. Then, drain polarization of transistor at V_{ds} = 80 mV allows an excellent compromise between noise performances and power dissipation.

5. Conclusion

In this study, we reported on microwave and noise performances in low-power regime of AlSb/InAs HEMTs with optimized heterostructure. Combined (f_T, $f_{\max}$) of (100 GHz, 125 GHz) have been obtained at V_{ds} = 80 mV and DC power consumption of 4 mW/mm, performances that cannot be reached at V_{ds} = 240 mV for such a low

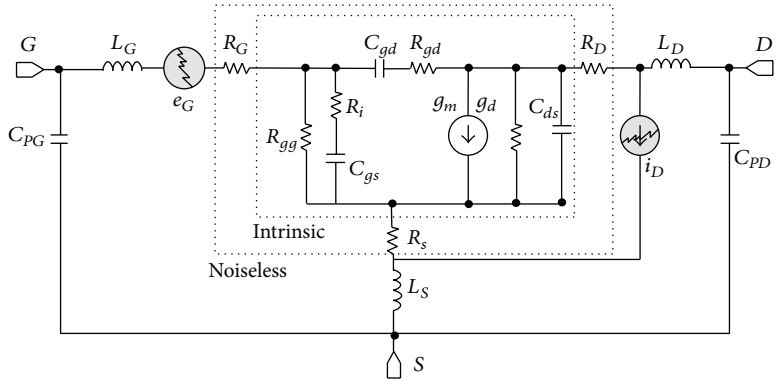

FIGURE 8: Small-signal equivalent circuit with noise sources for AlSb/InAs HEMT at V_{ds} = 80 mV.

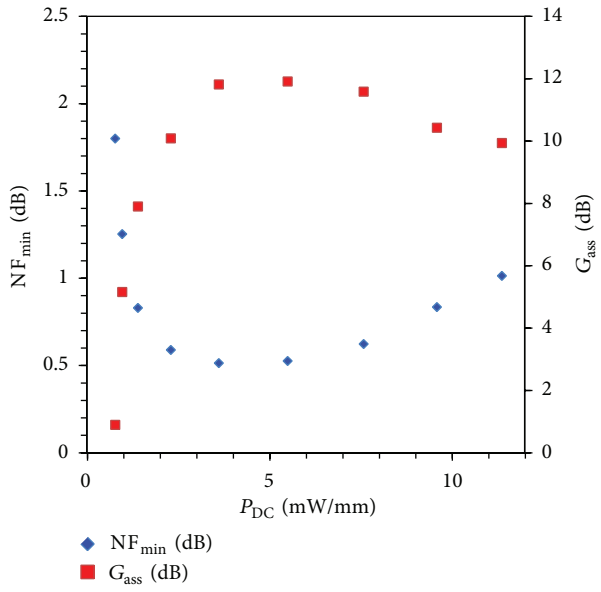

FIGURE 9: Minimum noise figure NF_{min} and associated gain G_{ass} as a function of power consumption at 12 GHz for V_{ds} = 80 mV.

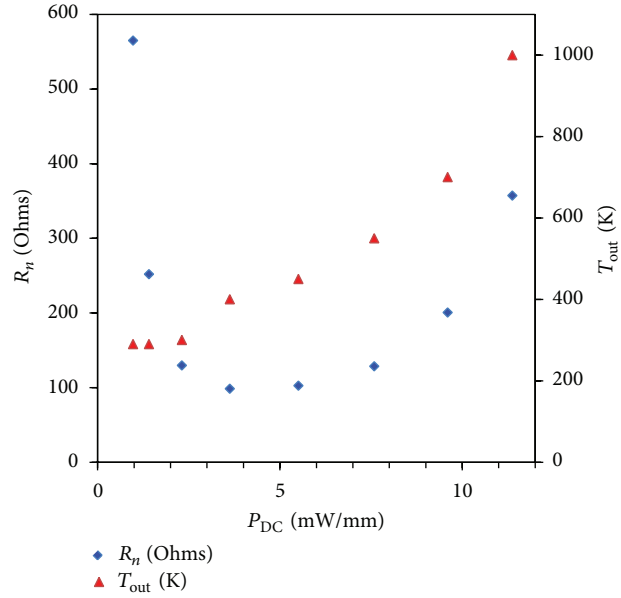

FIGURE 10: Noise equivalent resistance R_n and output noise temperature T_{out} as a function of power consumption at 12 GHz for V_{ds} = 80 mV.

power dissipation. A small-signal equivalent circuit was established and demonstrated that impact ionization effects at V_{ds} = 80 mV are negligible, which is not the case for V_{ds} = 240 mV. This allowed an accurate extraction of noise parameters thanks to SSEC with noise sources fully reliable in mobility regime. NF_{min} = 0.5 dB and G_{ass} = 12 dB have been obtained at 12 GHz for (V_{ds} = 80 mV; P_{DC} = 4 mW/mm). These results exhibit the high suitability of AlSb/InAs HEMTs for combined RF and low-noise performances in ultra-low-power dissipation regime.

Conflict of Interests

The authors declare that there is no conflict of interests regarding the publication of this paper.

Acknowledgments

This work is supported by the National Research Agency under Projects Low IQ (no. ANR-08-NANO-022) and SMIC (no. ANR-11-ASTR-031-03).

References

[1] W. Deal, X. B. Mei, K. M. K. H. Leong, V. Radisic, S. Sarkozy, and R. Lai, "THz monolithic integrated circuits using InP high electron mobility transistors," *IEEE Transactions on Terahertz Science and Technology*, vol. 1, no. 1, pp. 25–32, 2011.

[2] B. R. Bennett, R. Magno, J. B. Boos, W. Kruppa, and M. G. Ancona, "Antimonide-based compound semiconductors for electronic devices: a review," *Solid-State Electronics*, vol. 49, no. 12, pp. 1875–1895, 2005.

[3] C.-A. Chang, L. L. Chang, E. E. Mendez, M. S. Christie, and L. Esaki, "Electron densities in InAs-AlSb quantum wells," *Journal of Vacuum Science & Technology B*, vol. 2, no. 2, pp. 214–216, 1984.

[4] G. Tuttle and H. Kroemer, "An AlSb/InAs/AlSb quantum well HFT," *IEEE Transactions on Electron Devices*, vol. 34, no. 11, p. 2358, 1987.

[5] B. Y. Ma, J. Bergman, P. Chen et al., "InAs/AlSb HEMT and its application to ultra-low-power wideband high-gain low-noise amplifiers," *IEEE Transactions on Microwave Theory and Techniques*, vol. 54, no. 12, pp. 4448–4454, 2006.

[6] W. R. Deal, R. Tsai, M. D. Lange, J. Brad Boos, B. R. Bennett, and A. Gutierrez, "A low power/low noise MMIC amplifier for phased-array applications using InAs/AlSb HEMT," in *Proceedings of the IEEE MTT-S International Microwave Symposium Digest*, pp. 2051–2054, June 2006.

[7] Y. Roelens, A. Olivier, L. Desplanque et al., "Tellurium δ-doped 120 nm AlSb/InAs HEMTs: towards sub-100 mV electronics," in *Proceedings of the 68th Device Research Conference (DRC '10)*, pp. 53–54, June 2010.

[8] A. Olivier, A. Noudeviwa, N. Wichmann et al., "High frequency performance of tellurium δ-doped AlSb/InAs HEMTs at low power supply," in *Proceedings of the 5th Microwave Integrated Circuits Conference (EuMIC '10)*, pp. 162–165, Paris, France, October 2010.

[9] L. Desplanque, S. El Kazzi, J. Codron -L et al., "AlSb nucleation induced anisotropic electron mobility in AlSb/InAs HEMTs heterostructures on GaAs," *Applied Physics Letters*, vol. 100, no. 26, pp. 262103–262104, 2012.

[10] C. Gardès, S. M. Bagumako, L. Desplanque et al., "120 nm AlSb/InAs HEMT without gate recess: 290 GHz f_T and 335 GHz f_{max}," in *Proceedings of the International Conference on Indium Phosphide and Related Materials (IPRM '13)*, pp. 1–2, Kobe, Japan, 2013.

[11] Y. C. Chou, L. J. Lee, J. M. Yang et al., "The effect of gate metals on manufacturability of 0.1 μm metamorphic AlSb/InAs HEMTs for ultra low-power applications," in *Proceedings of the 20th International Conference on Indium Phosphide and Related Materials (IPRM '08)*, pp. 1–14, May 2008.

[12] R. Tsai, M. Lange, L. J. Lee et al., "260 GHz f_T, 280 GHz f_{max} AlSb/InAs HEMT technology," in *Proceedings of the 63rd Device Research Conference (DRC '05)*, pp. 257–258, June 2005.

[13] J. Brad Boos, W. Kruppa, B. R. Bennett et al., "AlSb/InAs HEMT's for low-voltage, high-speed applications," *IEEE Transactions on Electron Devices*, vol. 45, no. 9, pp. 1869–1875, 1998.

[14] G. Moschetti, M. Abbasi, Per-Ake Nilsson et al., "True planar InAs/AlSb HEMTs with ion-implantation technique for low-power cryogenic applications," *Solid-State Electronics*, vol. 79, pp. 268–273, 2013.

[15] C. Teyssandier, F. de Groote, R. Sommet et al., "Characterization and modeling of impact ionization effects on small and large signal characteristics of AlGaAs/GaInAs/GaAs PHEMTs," in *Proceedings of the 3rd European Microwave Integrated Circuit Conference (EuMIC '08)*, pp. 119–122, Amsterdam, The Netherlands, October 2008.

[16] M. Isler, "Investigation and modeling of impact ionization in HEMTs for DC and RF operating conditions," *Solid-State Electronics*, vol. 46, no. 10, pp. 1587–1593, 2002.

[17] G. Dambrine, H. Happy, F. Danneville, and A. Cappy, "New method for on wafer noise measurement," *IEEE Transactions on Microwave Theory and Techniques*, vol. 41, no. 3, pp. 375–381, 1993.

[18] R. Tsai, R. Grundbacher, M. Lange et al., "Manufacturable AlSb/InAs HEMT technology for ultra-low power millimeter-wave integrated circuits," in *Proceedings of the Mantech Conference*, pp. 69–72, 2004.